Cost-effective design of the alkaline electrolyser for enhanced electrochemical performance and reduced electrode degradation

Daniel Symes*, Bushra Al-Duri, Waldemar Bujalski and Aman Dhir
Centre for Hydrogen and Fuel Cell Research, School of Chemical Engineering, University of Birmingham, B15 2TT, UK

Abstract

An alkaline electrolyser was developed and characterized. Three different metals, working as the electrode, were analysed using electrochemical methods to determine the best electrochemical performance. The performance of the Stainless Steel (SS316) electrode and the nickel electrode is much better than that of the conventional iron electrode. Degradation analysis of the electrode materials highlighted the need for the material to be durable and resistant to corrosion from an alkaline environment. Through SEM and mass analysis, it is shown that Nickel exhibits the strongest long-term resistance to surface and electrochemical performance degradation, when compared with Mild Steel (Iron) and SS316.

Keywords: electrolyser; electrode degradation; electrolysis; water electrolysis; alkaline electrolyser

*Corresponding author:
dxs654@bham.ac.uk

Received 4 July 2012; revised 2 November 2012; accepted 29 March 2013

1 INTRODUCTION

The global demand of energy is leading to the inevitable shortage of fossil fuels, which is the primary resource for our energy requirements. Fossil fuels are formed by the anaerobic decomposition of dead organisms in the planet's crust and are a finite resource, which has led to increased research into new sources of energy. When they eventually become obsolete, we will have to get our energy from other sources [1].

A shift in focus to the production of energy from renewable resources has increased the public awareness of potential energy shortcomings due to depleting fossil fuel resources. Hydrogen is an effective energy carrier for renewable resources, and this energy can be extracted from hydrogen through fuel cells and internal combustion engines. Hydrogen can also be used for energy storage, for example, during off-peak hours, excess electrical energy, instead of being wasted, could be stored in the form of hydrogen via electrolysis [2].

Many academics believe that the only realistic way to produce hydrogen without creating any greenhouse gases is through the use of renewable energy sources. These include solar, wind and hydro energy sources. It is important to remember that hydrogen is an energy carrier, not a primary energy source [3].

Approximately 94% of current hydrogen is obtained from fossil fuels from a process called steam reforming. These processes produce greenhouse gases and do not produce as high a purity of hydrogen that water electrolysis produces [4].

Water electrolysis currently accounts for 4% of global hydrogen production and involves the passing of an electrical current through water-based solutions which produce hydrogen and oxygen as the only products, therefore no greenhouse gas emissions [5]. If the electricity supplied to the electrolysis cell comes from renewable resources, the whole process is carbon neutral, i.e. no greenhouse gas emissions.

Electrolysers use electrical current to split water into its constituents, and there are two main types of electrolysers, alkaline electrolysers and polymer electrolyte membrane (PEM) electrolysers.

Water has a very high electrical resistance and cannot be directly split into hydrogen and oxygen. This can only occur when extremely high electrical currents are applied to the system, which is impractical. Therefore, the addition of an electrolyte lowers the electrical energy required to initiate the reaction [6].

Alkaline electrolysers use a liquid electrolyte in the form of an acid/base/salt to produce hydrogen, whereas PEM electrolysers use a solid polymer electrolyte in the form of a membrane to

International Journal of Low-Carbon Technologies 2015, 10, 452–459
© The Author 2013. Published by Oxford University Press.
This is an Open Access article distributed under the terms of the Creative Commons Attribution Non-Commercial License (http://creativecommons.org/licenses/by-nc/3.0/), which permits non-commercial re-use, distribution, and reproduction in any medium, provided the original work is properly cited. For commercial re-use, please contact journals.permissions@oup.com
doi:10.1093/ijlct/ctt034 Advance Access Publication 27 May 2013

Downloaded from https://academic.oup.com/ijlct/article-abstract/10/4/452/2363372
by Russells Hall Hospital Learning Centre user
on 17 April 2018

split pure water into hydrogen and oxygen without the need for any harmful acids/alkalis [7].

This work herein examines the potential for improving an existing alkaline electrolyser from electrochemistry first principles by manipulating the electrodes.

2 THEORY

At standard temperature and pressure (S.T.P., 298 K, 1 atm), Gibbs free energy of formation is defined as a point of zero energy and is used to calculate the change in energy of a system. The open-circuit voltage (minimum) potential required electrolysing water into hydrogen and oxygen is determined by the change in Gibbs free energy of formation between reactants and products. Gibbs free energy changes with temperature and state (gas or liquid) [8]:

$$E_{\mathrm{o}} = \frac{\Delta G^{\mathrm{o}}}{zF} \tag{1}$$

where E_o is the theoretical minimum reversible potential of an electrolysis cell, z the number of electrons transferred in the reaction and F the Faraday number (96 485 Coulomb mol^{-1}).

At S.T.P., the Gibbs free energy of formation is +237.2 kJ mol^{-1}; therefore, $E_o = 1.23$ V. This is the minimum potential required to split water and produce hydrogen and oxygen. Under adiabatic conditions, the total enthalpy must be provided by the electrical energy [9]. In this case, the thermoneutral voltage is required to maintain the electrochemical reaction without heat generation.

The actual potential (E_{cell}) required to split water will require E_{cell} to be greater than E_o. The difference is known as overpotential, losses or polarization [10]. Thus, hydrogen evolution does not occur at the reversible potential (1.23 V). These are resistances in the cell that result in a higher potential being required to split water in order to overcome these resistances.

The electrical circuit analogy can be used to illustrate the various resistances encountered during the electrolysis process (Figure 1) [11].

There are three main types of resistance in the electrolysis cell: electrical resistances, transport resistances and electrochemical reaction resistances. These are shown below:

$$\begin{aligned} R_{\mathrm{cell}} = & R_1 + R_1' + R_{\mathrm{bubble,O_2}} + R_{\mathrm{bubble,H_2}} + R_{\mathrm{ions}} \\ & + R_{\mathrm{membrane}} + R_{\mathrm{anode}} + R_{\mathrm{cathode}} \end{aligned} \tag{2}$$

Electrical resistances (R_1 and R_1') directly result in heat generation which leads to the waste electrical energy in the form of heat according to Ohm's law. In water electrolysis, the forms of electrical resistance in the system are from the resistances in electrical circuits. The transfer of ions with the electrolyte depends on the electrolyte concentration (if liquid), membrane (if solid) and separation distance between the cathode and the anode [11]. The presence of bubbles on the electrode surfaces creates resistances to the ionic transfer and thus the electrochemical reaction.

The aims of this research are to increase mass transfer on the electrode surface. This, however, could hinder the production rate of hydrogen. Increasing mass transfer on the electrodes will create a larger volume of bubble formation. This additional bubble formation could reduce the contact area between the electrolyte and the electrode and therefore limit the number of active sites available for nucleation. One way to minimize this effect is by the circulation of electrolyte through the electrolyser. This mechanically removes bubbles from the electrode surface at a faster rate and therefore significantly reduce bubble overpotential in solution [12].

At equilibrium (open cell voltage), there exists dynamic currents, at each electrode and are a fundamental aspect of electrode behaviour. They are known as the cathode and anode exchange current density, which can be defined as the rate of reduction and oxidation, respectively. The exchange current density is a quantification of an electrode ability to transfer electrons and occurs in both directions equally, resulting in no change in composition of the electrode. When a small exchange current density exists, it represents slow reaction kinetics and a slow rate of electron transfer. A large exchange current density symbolizes fast reaction kinetics and a fast rate of electron transfer [13].

For the electrochemical reaction to proceed on an electrodes surface, an energy barrier must be overcome. This is the activation energy and results in activation overpotential in electrochemical reactions; these losses are irreversible. The activation overpotential is the additional voltage required to overcome the energy barrier of the rate determining the step of the electrochemical reaction to a value at which the reaction will proceed at a suitable rate [13].

3 METHODS

Electrochemical overpotential analysis was completed using a simple experimental procedure as shown in Figure 2. The electrodes of choice were placed 10 mm apart for each experiment, keeping the ohmic resistance constant. The electrolyte concentration was kept at 0.1 M KOH, maintaining the concentration overpotential constant. Consequently, by varying the electrode material, the only variation in electrochemical performance would be a result of the activation overpotential. The potation

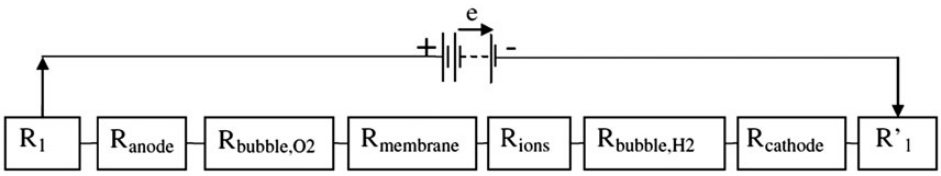

Figure 1. *Electrical circuit analogy of water electrolysis [11].*

Downloaded from https://academic.oup.com/ijlct/article-abstract/10/4/452/2363372
by Russells Hall Hospital Learning Centre user
on 17 April 2018

difference across the plates was supplied by Thurlby Thandar QPX1200L 1.2 kW.

The following electrode materials were tested (Table 1). Gas volume measurements were conducted using a gas syringe over a period of time to enable the volumetric flow rate to be calculated. Gas composition analysis was completed using a MKS instruments Minilab. Mass spectrometry (MS) is a measurement technique for the determination of the elemental composition of a molecule or compound. It is also used for interpreting the chemical structures of molecules. The MS principle consists of ionizing chemical compounds to generate charged molecules or molecule fragments and the measurement of their mass-to-charge ratios (*m/z*) [13].

4 STACK DESIGN AND DEVELOPMENT

From the defined project goals after analysis of the commercial initial unit, an objective was to increase the rate of hydrogen production from the electrolyser without increasing the footprint (size) of the electrolyser (2000 cm^3). Since the electrical input to the electrolyser would need to remain constant (12 V), it was clear that the surface area of electrodes would need to increase. From redesigning the electrolyser, it has been possible to increase the surface area from 600 to 5000 cm^2.

The new electrolyser design takes into account the need for no increase in footprint size and builds in the ability to hold up to 24 electrode plates (100 mm × 100 mm × 1 mm), with a 6-mm spacing between each plate. These 24 plates represent up to 12 electrolysis cells in the electrolyser stack.

The casing was custom built out of Perspex (10 mm thickness—for experimental purposes), which aided in bubble analysis into the reaction kinetics occurring in the electrolyser. Precision slots were machined, which allowed for ease of removal and modification of each electrode. The plates were connected in parallel using two stainless steel (SS316) bars (150 mm × 20 mm × 1 mm), which were connected to the electrodes using SS316 screws.

At one end of each interconnect was an SS316 screw soldered onto it for the electrical energy input to the electrolyser stack. These were accompanied with two 3/8″ ID nylon nozzles which were placed symmetrically central in the electrolyser lid for the connection of the stack to the electrolyte reservoir.

Figure 3 shows the design of the electrolyser with 6 mm separation distance between the electrodes. This small distance should limit the quantity of ohmic resistance exhibited in the electrolyser. No separator was used in the design of the electrolyser, since there is no requirement for the hydrogen and oxygen gas to be separated for the end application. This enabled maximization of the electrode surface area in the electrolyser cell. The constructed electrolyser is shown in Figure 4.

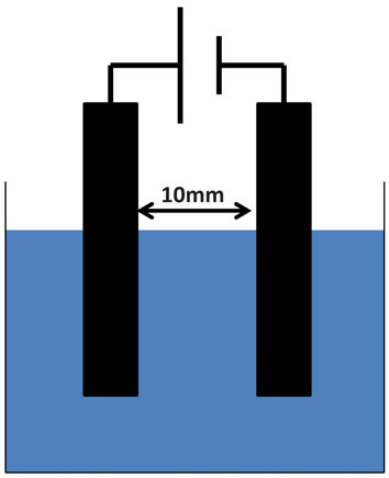

Figure 2. *Experimental setup.*

Table 1. *Electrode materials and properties*

Material	Cost (metal exchange as of 21 October 2011)	Electrical resistivity in literature (20°C)	References
Pt (platinized)	£31 400/kg	105 nΩ m	[14–17]
Palladium	£12 350/kg	105.4 nΩ m	[14, 18]
Gold	£34 144/kg	22.14 nΩ m	[11, 19]
Iron	£2.81/kg	96.1 nΩ m	[13, 16]
Pt (shiny)	£31 400/kg	105 nΩ m	[14–17]
Silver	£717.83/kg	15.87 nΩ m	[13, 16]
Nickel	£17.40/kg	69.3 nΩ m	[8, 20]
Graphite	£21.10/kg	7800 nΩ m	[21–23]
Lead	£4.05/kg	208 nΩ m	[13]
SS316	£3.86/kg	100 nΩ m	[16, 20]
Magnesium	£5.62/kg	43.9 nΩ m	[11, 13]
Titanium	£11.95/kg	420 nΩ m	[24]
Copper	£4.13/kg	16.78 nΩ m	[11, 13]
Aluminium	£1.65/kg	28.2 nΩ m	[16, 20]
Tin	£17.17/kg	115 nΩ m	[11, 16]
Zinc	£1.18/kg	59 nΩ m	[13]

5 RESULTS

5.1 Material cost analysis

The electrochemical performance was plotted as a function of material cost for each electrode material highlighted in Table 1. The results are shown in Figure 5.

From calculating the decomposition potential for each electrode from their respective current–voltage curve and then plotting this as a function of the material cost, it can be seen that cheaper metals such as zinc, iron and brass exhibit cost-effective electrochemical behaviour.

5.2 Current density analysis

Further material characterization was completed by applying a potential of 12 V. From which the current per unit area (current density) was calculated. The results are shown in Figure 6.

Figure 6 shows that silver exhibits the best electrical conductivity (within the material set selected) at 12 V. Silver, however, is extremely expensive (Table 1) and is not economically viable for a 1.2-kw electrolyser design. The next three materials which exhibit good electrical conductivity are Iron (Mild Steel), Nickel

Downloaded from https://academic.oup.com/ijlct/article-abstract/10/4/452/2363372
by Russells Hall Hospital Learning Centre user
on 17 April 2018

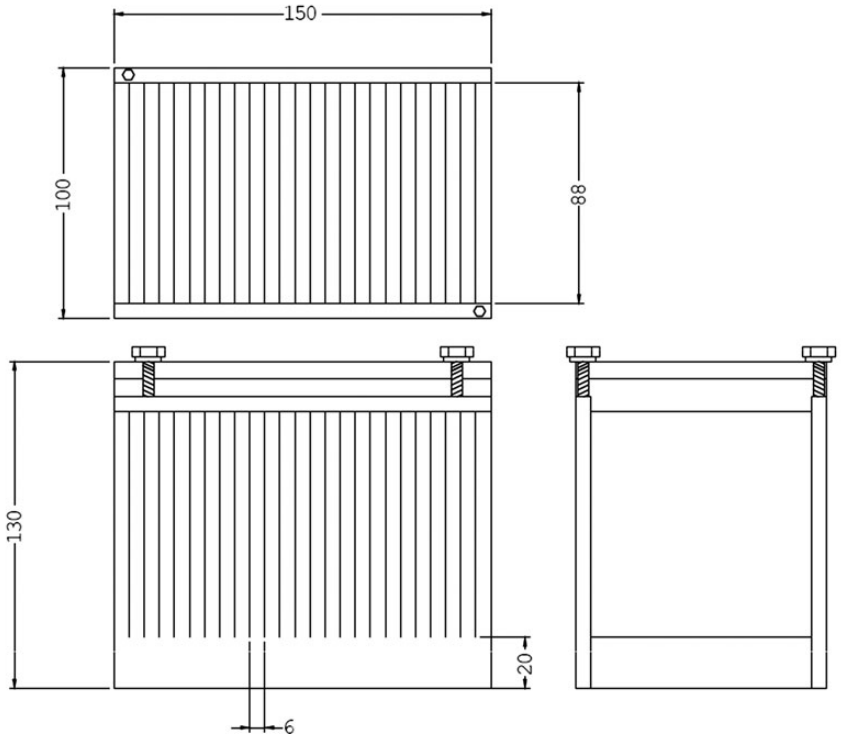

Figure 3. *CAD schematic of the electrolyser design.*

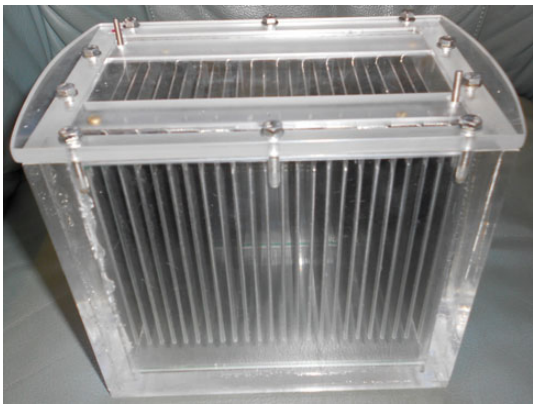

Figure 4. *Image of the constructed electrolyser.*

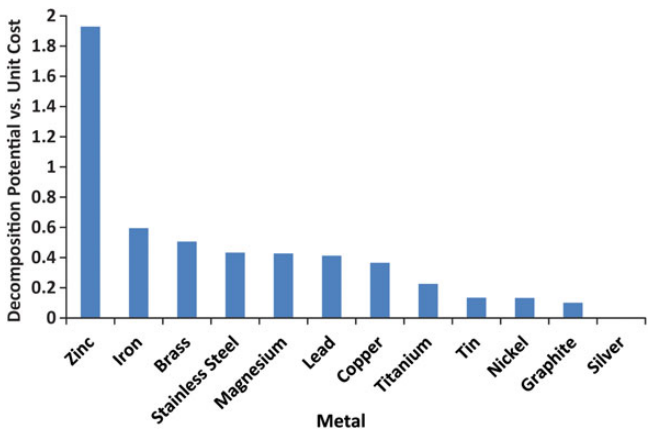

Figure 5. *Decomposition potential of electrode materials as a function of material cost.*

and Stainless Steel (SS316). As well as having good conductivity, all three materials have economical unit costs.

Two potential electrode materials, SS316 and nickel, were selected for further stack testing and analysis. These were tested in two modes, polished and unpolished. Unpolished was no surface treatment, and polished which had been treated with metal polish (Brasso).

5.3 Stack analysis

This was conducted for SS316 and Nickel plates. Figure 7 shows that for the same footprint there has been an increase in current flow for the same potential. At 4 V, there has been a 1500% increase from the commercial electrolyser to the improved design presented here. This does not take into account the surface area of the electrodes, where in this case this analysis is carried out for 24× SS316 plates and 20× Nickel plates.

This drastic increase in current flow has been attributed to the increase in the surface area of electrode (600 → 5000 cm^2). To analyse this further, we can electrochemically characterize the electrolyser stacks as a function of the electrode surface area (current density). This is shown in Figure 8.

Figure 8 shows a smaller enhancement in current density at a fixed potential. At 4 V, there is a 267% increase in performance from the commercial electrolyser to the new design for both

Downloaded from https://academic.oup.com/ijlct/article-abstract/10/4/452/2363372
by Russells Hall Hospital Learning Centre user
on 17 April 2018

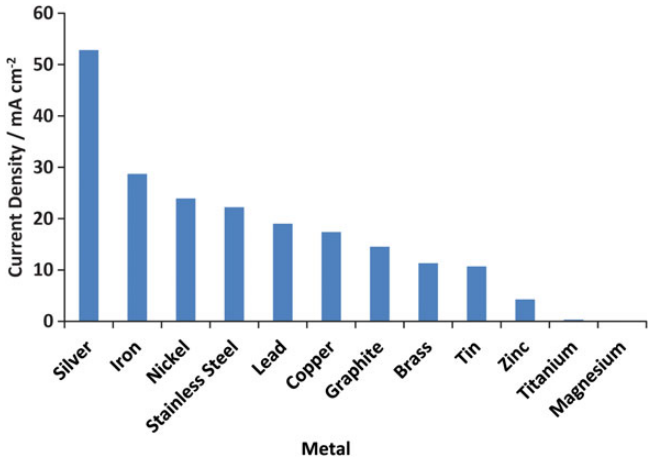

Figure 6. *Current density of electrode materials at 12 V.*

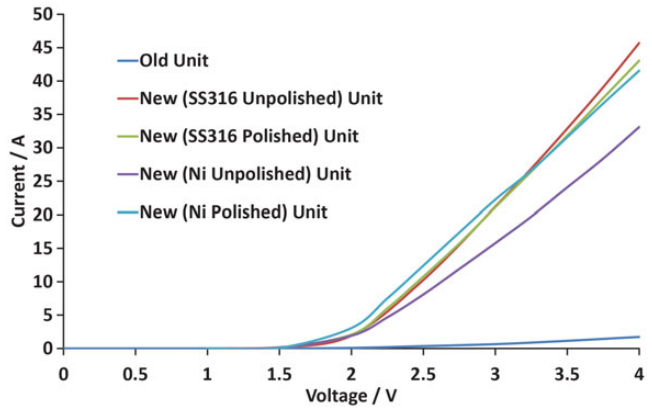

Figure 7. *Electrolyser current comparison using 0.1 M KOH solution.*

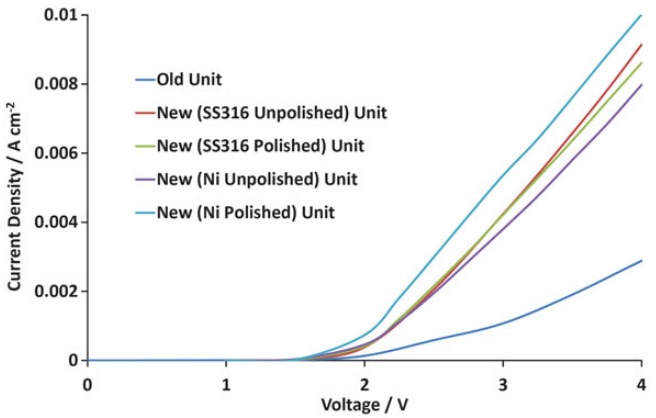

Figure 8. *Electrolyser current density comparison using 0.1 M KOH solution.*

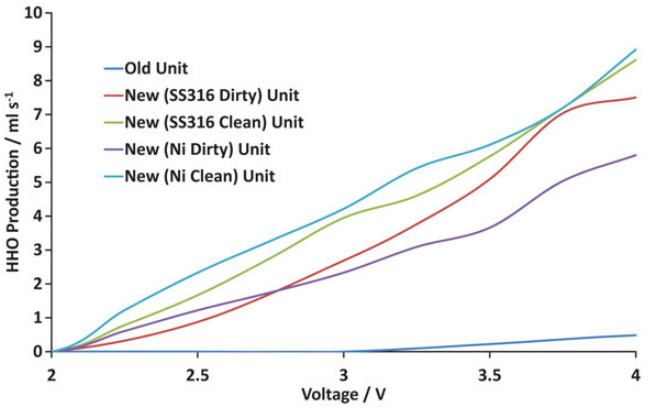

Figure 9. *Electrolyser HHO production comparison at 0.1 M KOH solution.*

electrode materials. This enhancement observed can be attributed to the decrease in resistance in the electrolyser system. It is believed the reduction in resistance is a result of the smaller separation distance between the electrodes (reducing the ohmic resistance), and the removal of 'neutral' plates in the electrolyser which prevent short circuits, but increased the resistance in the commercial electrolyser.

5.4 Gas productivity

The gas productivity of the electrolysers was also analysed. It is known that gas production rates are directly proportional to current flow according to Faraday's first law of electrolysis. Consequently, the gas production rate increases with an increasing potential.

Figure 9 shows the comparison in gas productivity from the commercial electrolyser to the new design. This increase at 4 V from $\sim$0.5 ml s^{-1} to 5 ml s^{-1}, a 10-fold increase. It also shows the polished (clean) electrode surfaces exhibit a higher gas production rate than the unpolished (dirty) electrode surfaces. This is a result of decreased surface tension (smoother electrode surfaces from a polishing process) which results in the removal of the oxide layer of the electrode, resulting in the increase in the electrode surface area for bubble nucleation. The increase in gas productivity from electrode surface polishing can also be attributed to oxide layer removal. Oxide layers increase resistance in the electrolyser, since it limits the number of active reaction sites available for bubble nucleation.

5.5 Current density vs. HHO production: Faraday's law of electrolysis

Current flow per unit surface area is directly proportional to the rate of gas evolution. This is Faraday's first law of electrolysis. Figure 10 shows this relationship as recorded from the improved electrolyser, for both electrode materials and surface characteristics.

The graph shows the directly proportional relationship between current density and gas productivity. To achieve the clearly set objectives of 4LPM HHO gas for effective catalytic behaviour in the combustion engine, a large current density is required to meet these flow rates. This can be achieved by increasing the concentration of KOH solution, which conversely increases the rate of electrode degradation, by increasing the potential applied to the electrolyser or increasing the electrode surface area further.

Downloaded from https://academic.oup.com/ijlct/article-abstract/10/4/452/2363372
by Russells Hall Hospital Learning Centre user
on 17 April 2018

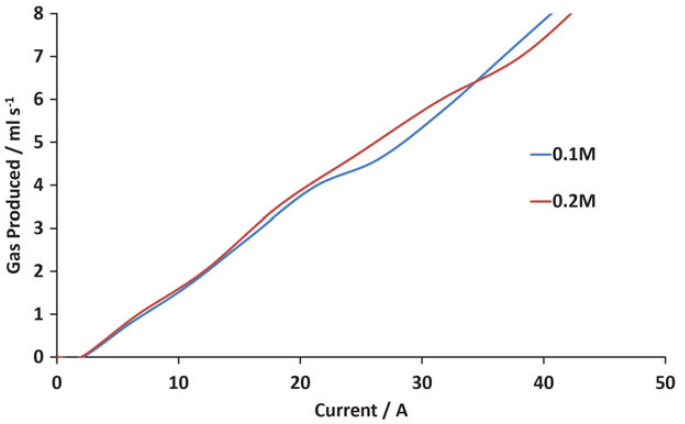

Figure 10. *Illustration of the linear relationship between gas evolution and electrical current.*

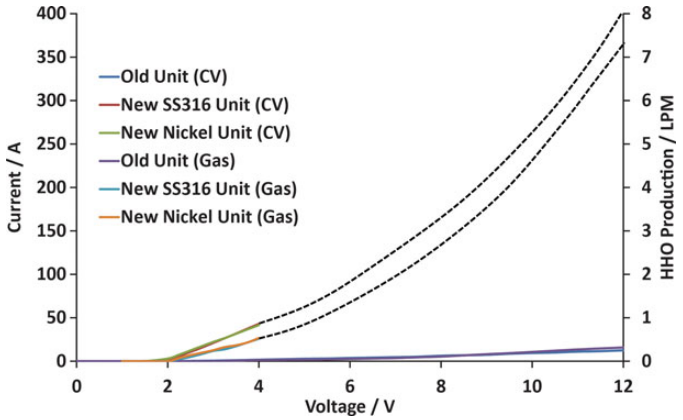

Figure 11. *Electrolyser current and HHO production projections at 0.1 M KOH solution.*

5.6 Performance projections

Equipment limitations meant that the operating current has been limited to 50 A. As a result, the operating potential has only been able to achieve 4 V. From the linear relationship between voltage and current and gas productivity, the data can be extrapolated up to 12 V and a projection can be made on the resultant current and HHO gas production. This is shown in Figure 11.

Assuming the electrolyser behaves as previous electrolyser cells tested, the approximate current expected at 12 V is 400 A, while this should result in a HHO gas flow rate of 8 LPM.

5.7 Mass spectroscopy

Figure 12 illustrates the gas composition for the electrolyser gas outlet at 2 V and 1 ml s^{-1} of the gas flow rate.

The cycle was allowed to run on pure helium for 5 min, before being switched onto the electrolyser outlet feed. This gives us a static background reading of the air currently in the gas line and the electrolyser reservoir (as seen by the increase in Nitrogen N_2). After 10 min, the electrolyser is turned on and hydrogen is seen to be produced. At this point, the level of nitrogen in the system decreases and the oxygen level increases further (as a result of being produced from the electrolyser).

After ∼100 min, the system reaches an equilibrium where there is 60% oxygen and 30% hydrogen gas percentage in the electrolyser outlet. There is also a small proportion of water present (vapour carry over from the electrolyser).

5.8 Degradation studies

The lifetime of the electrolyser needs to be maintained, so it achieves the specified 250 h operation. To analyse this further, the rates of degradation were studied in *in situ* (in the electrolysis mode). These processes involve the application of metal polish to the electrodes and the electrochemical performance as a result of the metal polish, and the current degradation analysis of the electrolyser over a fixed period of time.

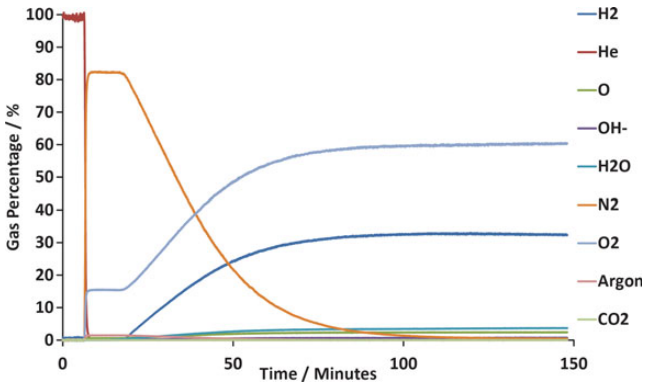

Figure 12. *Gas composition analysis of gas produced from the electrolyser.*

5.8.1 *Stack lifetime*

To analyse the performance of the electrolyser lifetime, the current variation can be measured at a fixed potential over time. Figure 13 shows the current degradation in the electrolyser for SS316 and Nickel for a period of 7 h.

Figure 13 shows that there is a decrease in current flow over the 7 h of operation, seen by the negative gradient for the two electrode materials. The current decreases by 11% for the SS316 and 3% for the Nickel over the 7 h.

Using the gradient of the data points, it can be approximated that the time it takes until zero current occurs assuming that the rate of degradation remains constant. For SS316, this is ∼53 h, and for Nickel, this is 242 h. A 5-fold lifetime extension can be found for using Nickel electrodes instead of SS316.

5.8.2 *Electrode surface cleaning*

To increase the lifetime of the electrolyser, the application of metal polish on the surface of the electrodes was investigated. The polishing of the plates should theoretically remove the oxide layers formed on the plates due to exposure to alkaline solution. This reduces the resistance in the electrolyser unit. The change in appearance between an unpolished (top) and a polished (bottom) plate can be seen in Figure 14. The cleaner surface is

Downloaded from https://academic.oup.com/ijlct/article-abstract/10/4/452/2363372
by Russells Hall Hospital Learning Centre user
on 17 April 2018

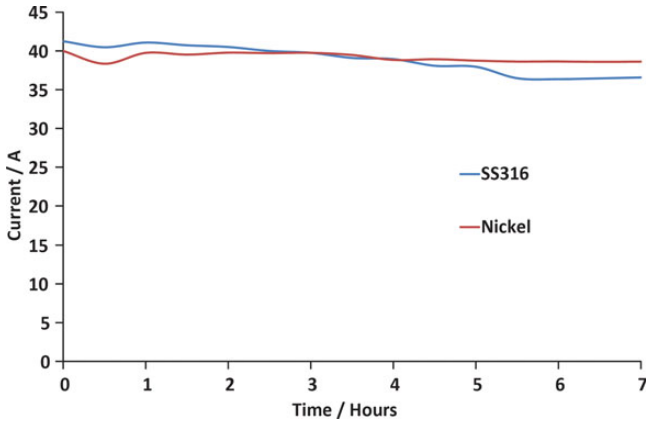

Figure 13. *Current degradation at fixed potential (4 V).*

expected to give rise to a higher rate of bubble evolution due to more active reaction sites available on the electrode surface area.

An analysis of the effect that polishing the plates has on Nickel is presented in Figure 15. It shows for two different concentrations that polishing the plates increases the flow of current between the plates and subsequently increases the rate of HHO gas production for varying potentials.

From this analysis, the benefits of electrode surface cleaning are evident. This can be characterized further by conducting a current degradation evaluation to illustrate how the current decreases over time due to an increase in resistance in the electrolyser cell. This will be carried out over an 8-h period, then switched off and leaving the KOH solution in the electrolyser overnight (16 h), and then turning the power on for another 3 h the following day. After this, the electrodes are then polished (removal of the oxide layer) and the current degradation was continued at a fixed potential for a further 3 h. This was completed for two fixed potentials and is shown in Figure 16.

Figure 16 shows the long-term electrolytic behaviour of the electrolyser incorporating electrode cleaning and systematic 'no power' periods to simulate the real-world application of this electrolyser.

There are three main behaviour patterns in Figure 16. The first shows a steady increase in current over time during start up. This is due to the increasing temperature of the electrolyte, which allows the ions to move more freely. Second, once the electrolyte temperature has achieved equilibrium, the current starts to slowly decrease due to the build up of oxide layers on the surface of the electrodes. This limits the number of nucleation sites available for the electrochemical reaction.

Third, after the electrolyser was shutdown and left sitting in solution for 3 h, the power was reintroduced to the electrolyser and a decrease in current was observed from 3 h previously when the electrolyser was at equilibrium operating temperature, which is now at room temperature. The data show the current flow increases at a slower rate than seen before due to the presence of the recently formed oxide layers in the first cycle of testing.

Left for an extended period of 15 h in the shutdown mode and the electrolyte still present in the electrolyser, the expected increase in the size of the oxide layer is expected to result in a decrease in current flow further. Reducing the formation of the oxide layer on the electrode is imperative to the lifetime and electrochemical performance of the alkaline electrolyser.

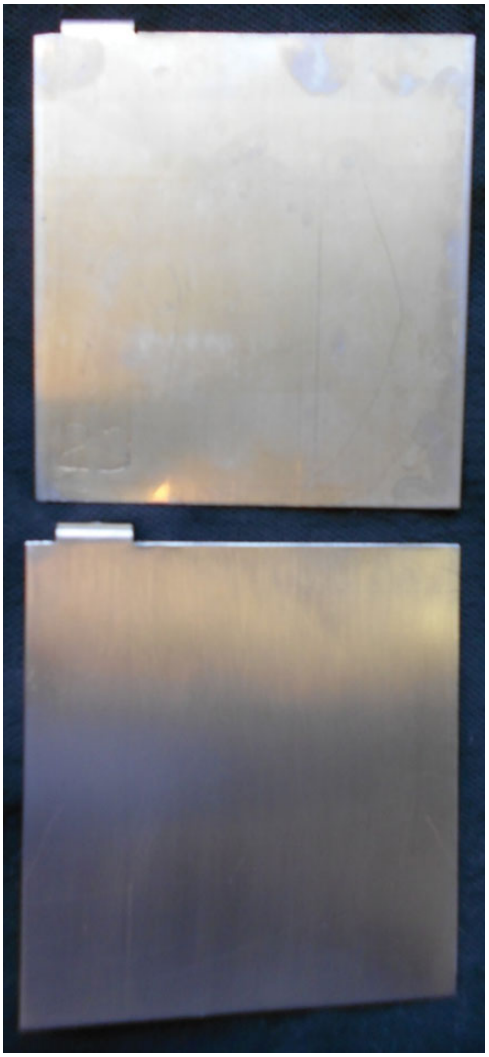

Figure 14. *Image of an unpolished plate (top) and a polished plate (bottom).*

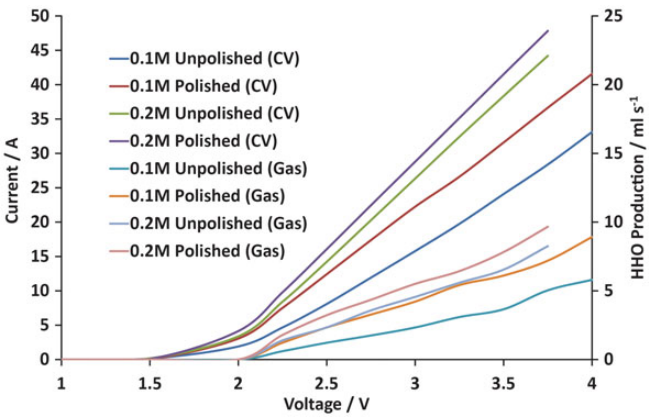

Figure 15. *Electrochemical performance comparison for unpolished and polished Nickel plates.*

Downloaded from https://academic.oup.com/ijlct/article-abstract/10/4/452/2363372
by Russells Hall Hospital Learning Centre user
on 17 April 2018

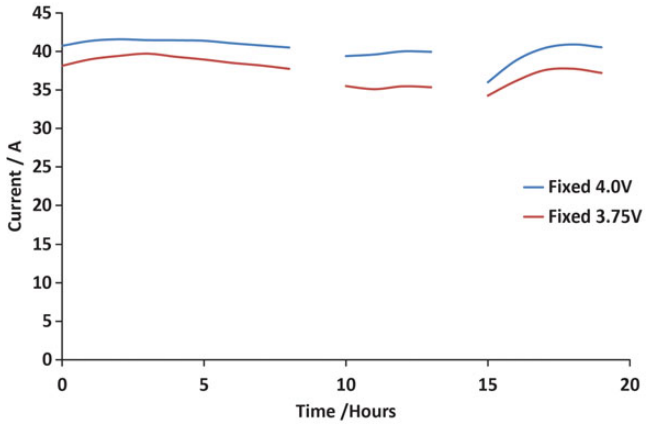

Figure 16. *Current degradation cycling testing.*

6 CONCLUSIONS

This paper explains the development and characterization of an alkaline electrolyser produced for transportation purposes. Its goal is to produce at least 4 LPM of HHO gas, using cost-effective materials for the electrochemical reaction.

A number of electrode materials were selected and tested to find a material which has high electrochemical performance and is cost effective. Taking into account the cost of each electrode material, they were each tested at a fixed potential (12 V) and current recorded to see which metal produced the highest current. Iron, Stainless Steel and Nickel represent the best performance to cost ratio from this experimental data.

These three metals were then analysed using electrochemical techniques to determine the best electrochemical performance and least surface degradation impacts. Stainless Steel and Nickel both exhibited good electrochemical performance, with the latter exhibiting no visual surface degradation when subjected to an alkaline environment.

Electrochemical performance testing over extended periods of time discovered the formation of an oxide layer on the surface of the electrodes, and the degradation in current flow over time was quantified. A method for the removal of the oxide layer and the subsequent characterization of the electrodes with and without the oxide highlighted the increased electrochemical performance when the oxide layer is removed.

An alkaline electrolyser was built using Nickel plates, which was characterized up to a potential of 4 V for bench testing, and projections were made for electrochemical performance at 12 V, of which is expectant to be ∼400 A.

ACKNOWLEDGEMENTS

I would like to take this opportunity to thank supervisors and colleagues at the Centre for Hydrogen and Fuel Cell Research, University Birmingham, UK. I would also like to thank the Engineering and Physical Sciences Research Council for funding my PhD as part of the Doctoral Training Centre in Hydrogen, Fuel Cells and their Applications.

REFERENCES

[1] Zoulias E, Varkaraki E, Lymberopoulos N, *et al.* A review of water electrolysis. *TCJST* 2004;**4**:41–71.
[2] Stojic D. Hydrogen generation from water electrolysis—possibilities of energy saving. *J Power Sources* 2003;**118**:315–9.
[3] Grigoriev S, Porembsky V, Fateev V. Pure hydrogen production by PEM electrolysis for hydrogen energy. *Int J Hydrogen Energy* 2006;**31**:171–5.
[4] Marbán G, Valdés-Solís T. Towards the hydrogen economy? *Int J Hydrogen Energy* 2007;**32**:1625–37.
[5] Marshall A, Børresen B, Hagen G, *et al.* Hydrogen production by advanced proton exchange membrane (PEM) water electrolysers—Reduced energy consumption by improved electrocatalysis. *Energy* 2007;**32**:431–6.
[6] Gupta RB. *Hydrogen Fuel, Production, Transport and Storage.* CRC Press, 2008.
[7] Wei G, Wang Y, Huang C, *et al.* The stability of MEA in SPE water electrolysis for hydrogen production. *Int J Hydrogen Energy* 2010;**35**:3951–7.
[8] Ganley JC. High temperature and pressure alkaline electrolysis. *Int J Hydrogen Energy* 2009;**34**:3604–11.
[9] Choi P. A simple model for solid polymer electrolyte (SPE) water electrolysis. *Solid State Ionics* 2004;**175**:535–9.
[10] Harrison K, Levene JI. *Electrolysis of Water.* National Renewable Energy Laboratories, 2004.
[11] Zeng K, Zhang D. Recent progress in alkaline water electrolysis for hydrogen production and applications. *Prog Energy Combust Sci* 2010;**36**:307–26.
[12] O'Brien JE, McKellar MG, Stoots CM, *et al.* Parametric study of large-scale production of syngas via high-temperature co-electrolysis. *International Journal of Hydrogen Energy* 2009;**34**:4216–26.
[13] Lee TS. Hydrogen over potential on pure metals in alkaline solution. *J Electrochem Soc* 1971;**118**:1278–82.
[14] Grigoriev SA, Mamat MS, Dzhus KA, *et al.* Platinum and palladium nanoparticles supported by graphitic nano-fibers as catalysts for PEM water electrolysis. *Int J Hydrogen Energy* 2010;**36**:4143–7.
[15] Millet P, Mbemba N, Grigoriev SA, *et al.* Electrochemical performances of PEM water electrolysis cells and perspectives. *International Journal of Hydrogen Energy* 2011;**36**:4134–42.
[16] Yazici B, Tatli G, Galip H, *et al.* Investigation of suitable cathodes for the production of hydrogen gas by electrolysis. *Int J Hydrogen Energy* 1995;**20**:957–65.
[17] Zhou L, Cheng Y. Catalytic electrolysis of ammonia on platinum in alkaline solution for hydrogen generation. *Int J Hydrogen Energy* 2008;**33**:5897–904.
[18] Huang Y-X, Liu XW, Sun XF, *et al.* A new cathodic electrode deposit with palladium nanoparticles for cost-effective hydrogen production in a microbial electrolysis cell. *Int J Hydrogen Energy* 2011;**36**:2773–6.
[19] Khanova LA, Krishtalik LI. Kinetics of the hydrogen evolution reaction on gold electrode. A new case of the barrierless discharge. *J Electroanal Chem* 2011;**660**:224–9.
[20] Bowen CT, Davis HJ, Henshaw BF, *et al.* Developments in advanced alkaline water electrolysis. *Int J Hydrogen Energy* 1984;**9**:59–66.
[21] Dubey PK, Sinha ASK, Talapatra S, *et al.* Hydrogen generation by water electrolysis using carbon nanotube anode. *Int J Hydrogen Energy* 2010; **35**:3945–50.
[22] Shi K, Hu Kun, Wang Sheng, *et al.* Structural studies of electrochemically activated glassy carbon electrode: Effects of chloride anion on the redox responses of copper deposition. *Electrochim Acta* 2007;**52**:5907–13.
[23] Wei ZD, Ji MB, Chen SG, *et al.* Water electrolysis on carbon electrodes enhanced by surfactant. *Electrochim Acta* 2007;**52**:3323–9.
[24] Ye F, Wang X, *et al.* Electrocatalytic properties of Ti/Pt-IrO2 anode for oxygen evolution in PEM water electrolysis. *Int J Hydrogen Energy* 2010;**35**:8049–55.

Downloaded from https://academic.oup.com/ijlct/article-abstract/10/4/452/2363372
by Russells Hall Hospital Learning Centre user
on 17 April 2018